Reconstruction of High-Frequency Lunar Digital Elevation Model using Shape from Shading

Min-Hyun CHO*,[1], Min-Jea TAHK[1]

*Corresponding author
[1]Korea Advanced Institute of Science and Technology (KAIST),
291, Daehak-ro, Yuseong-gu, Daejeon, 34141, Republic of Korea,
mhcho@fdcl.kaist.ac.kr *, mjtahk317@gmail.com

DOI: 10.13111/2066-8201.2018.10.1.2

Received: 21 November 2017/ Accepted: 19 January 2018/ Published: March 2018

Aerospace Europe CEAS 2017 Conference,
16th-20th October 2017, Palace of the Parliament, Bucharest, Romania
Technical Session Mission Design and Space Systems

Abstract: *This paper deals with a procedure to reconstruct a lunar surface based on fusion of Shape from Shading with absolute depth information exploited from Lunar Orbiter Laser Altimeter data. The generation of accurate lunar digital elevation model which contains altitude and terrain shape of mission area is critical for lunar exploration mission design. The photoclinometric approach with Shape from Shading yields dense, high-frequency information while range scanning data from Lunar Orbiter Laser Altimeter complements the photoclinometric reconstruction with low-frequency, large scale reliable depth information. The proposed Shape from Shading algorithm utilizes the laser altimetry data as initial guess and iteratively calculates the high-frequency altitude information from high resolution image. The high-frequency depth variation caused by small crater and boulder is recovered by applying Shape from Shading.*

Key Words: *High-Frequency Lunar Digital Elevation Model, Shape from Shading, Lunar Orbiter Laser Altimeter(LOLA) Data, Surface Reconstruction*

1. INTRODUCTION

The construction of Lunar Digital Elevation Model (LDEM) is essential for lunar exploratory mission. The DEM of lunar surface gives critical information during the various phase of lunar mission design, such as selection of candidates of lunar landing sites or implementation of Autonomous Landing and Hazard Avoidance Technology (ALHAT). There have been many studies related to the generation of lunar DEM. For instance, the NASA Ames Stereo Pipeline recovers three dimensional lunar surface from orbiter imagery [1]. The depth information of lunar surface can be estimated in many ways. As an example, NASA has been operated the Lunar Reconnaissance Orbiter (LRO) for years. Lunar Orbiter Laser Altimeter (LOLA) equipped on the LRO measures the depth information over lunar surface with range scanning [2]. The LOLA range scanning data covers large area of lunar surface while yielding reliable absolute depth reports. However, the LOLA range data is limited in the accuracy and resolution owing to laser altimeter performance and position uncertainty of LRO. To overcome the limitation of laser altimetry, two methods using images are proposed and studied widely.

The first method, photogrammetry (or triangulation), uses stereo image pairs to recover the depth information. Stereo photogrammetric approach requires stereo images over a target area and is capable of generate DEM with best resolutions of about three times of original stereo image. Since photogrammetric approaches are based on the difference of stereo image pair, the main focus of this approach is on conjugating image geometry with camera pose. Implementation and depth analysis is quite intuitive. Yet, the stereo image pair is a prerequisite and the data set is limited on the high resolution stereo image pair collected by the stereo LRO Camera (LROC). The LROC wide angle camera (WAC) has taken stereo reflectance images until it starts the mission and Global Lunar DTM 100m (GLD100) is turned out from LRO WAC data [3]. The photogrammetry is also applied to LROC narrow angle camera (NAC) images to produce high precision DEM [4].

The second approach, photoclinometry, reconstruct the DEM using the reflectance information and image photometric content. The photoclinometry can utilize the information captured in every pixel [10]. Although the photoclinmetry shows drawbacks of instability and ambiguity originated from its undetermined nature, the photoclinometry complements the existing DEM production method. While photogrammetry and LOLA data presents reliable and accurate DEM on large scales, the photoclinometric approach provides a pixel-wise depth variation and is able to recover the high-frequency information over the terrain which is extremely important for lunar mission design.

The Shape from Shading (SfS) or Shape and Albedo from Shading (SAfS) [7] is another name of photoclinometry. The Shape from Shading algorithm has advantage on that the shape information can be rebuilt from monocular image whereas stereo images are required for the photogrammetry. Since Shape from Shading handles pixel-wise reflectance information, a subtle change in depth caused by small crater and boulder can be captured and reflected to the DEM.

In this paper, the method for obtaining the high-frequency LDEM over lunar surface using Shape from Shading and Shape, Albedo from Shading are presented. The methods are implemented to refine an existing low resolution DEM from LOLA data to image pixel-level resolution DEM by reflectance-based reconstruction. In the section 2, the shape from shading algorithm for reconstructing DEM is described. Two methods, SfS and SAfS, are described. Section 3 shows LRO NAC image set for the surface reconstruction and explains how the LOLA data over interested region is attained. In section 4, the surface reconstruction results from two methods are presented. The analysis on surface refinement is given in last section.

2. PHOTOCLINOMETRIC APPROACH (SHAPE FROM SHADING)

Shape from Shading based on linear approximation

Photoclinometry calculates shape using a lighting equation, which considers the surface normal and lightening information to irradiance. The shape from shading usually uses monocular image as an input and constructs the depth information based on the surface orientation. It can also utilizes multiple images to reconstruct the depth information, which is called as photometric stereo. However, we are focusing on the surface refinement of the low resolution DEM. The shape from shading for only single image is considered.

In the shape from shading, the illumination direction information is prerequisite. The illumination direction given in the image should be converted into the quantity properly used for shape from shading. The illumination direction vector is calculated from the subsolar

azimuth angle and solar incidence angle. Since the absolute time, spacecraft position and relative position of sun and moon are recorded as kernel file when NAC image is taken, the subsolar azimuth angle and solar incidence angle can be retrieved from the mission data. The calculation of subsolar azimuth angle and incidence angle is implemented by post-mission data analysis program SPICE, including help with correlation of individual instrument data sets with those from other instruments on the same or on other spacecraft.

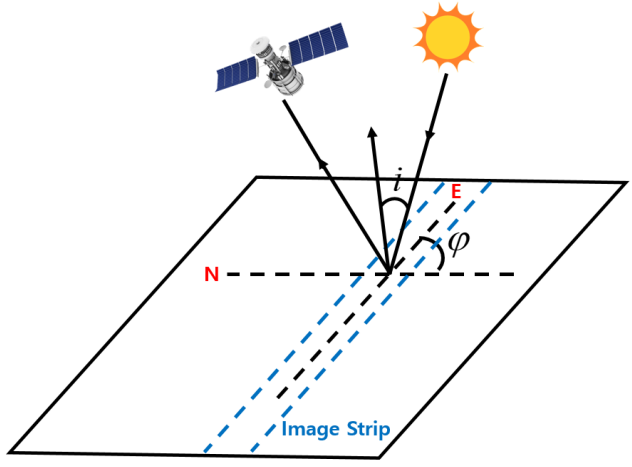

Fig. 1 – Image Illumination Geometry

For calculated subsolar azimuth angle φ and solar incidence angle i, the illumination direction is given as (1).

$$\begin{aligned} i_x &= \cos\left(\frac{\pi}{2} - i\right)\cos\varphi \\ i_y &= \cos\left(\frac{\pi}{2} - i\right)\sin\varphi \\ i_z &= \sin\left(\frac{\pi}{2} - i\right) \end{aligned} \tag{1}$$

Then, the slant angle and tilt angle of illumination defined on the image is specified as (2).

$$\begin{aligned} \sigma &= \cos^{-1}(i_z) \qquad & \sigma \in [0, \pi/2] \\ \tau &= \tan^{-1}\left(\frac{i_y}{i_z}\right) \qquad & \tau \in [0, 2\pi] \end{aligned} \tag{2}$$

There are many ways to implement Shape from Shading [5, 6]. In this paper, Shape from Shading using a linear approximation suggested by Shah et al [6] is used. The reconstructed terrain model is expressed in depth Z and gradient (p, q). The linear equations with three unknowns and nonlinear equation with two unknowns need to be solved. The reflectance map of lunar surface is assumed to be Lambertian surface whose luminance is not varying with viewing angle. The Shah's method is special case of minimizing multiscale generalized problem given as (3). The first term in (3) means a brightness constraint and second term means a smoothness constraint. The shape from shading with global minimization approach minimizes the cost functional given in (3).

$$\iint \sum_k [(E(x,y) - R(p,q))^2 + \lambda(p_x^2 + p_y^2 + q_x^2 + q_y^2)]dxdy \tag{3}$$

In Shah's approach, not only the Lambertian surface assumption but also the uniform albedo over the surface is assumed. Then, it is possible to express the image intensity as solely function of topological reflectance. The Shah's approach is simply minimizing the functional (3) by linearizing a depth map. For the image intensity, the reflectance is function of surface normal vector as (4).

$$I(x,y) = R(p,q) = \frac{\cos\sigma + p\cos\tau\sin\sigma + q\sin\tau\sin\sigma}{\sqrt{1+p^2+q^2}} \tag{4}$$

Using the following discrete approximations for surface normal as (5), the reflectance equation can be expressed as (6).

$$\begin{aligned} p &= \frac{\partial Z}{\partial x} = Z(x,y) - Z(x-1,y) \\ q &= \frac{\partial Z}{\partial y} = Z(x,y) - Z(x,y-1) \end{aligned} \tag{5}$$

$$\begin{aligned} 0 &= f(E(x,y), Z(x,\mathrm{y}), Z(x-1,\mathrm{y}), Z(x,\mathrm{y}-1)) \\ &= E(x,y) - R(Z(x,\mathrm{y}) - Z(x-1,\mathrm{y}), Z(x,\mathrm{y}) - Z(x,\mathrm{y}-1)) \end{aligned} \tag{6}$$

The linear approximation is applied to (6).

$$\begin{aligned} 0 &= f(E(x,y), Z(x,y), Z(x-1,y), Z(x,y-1)) \\ &\approx f(E(x,y), Z^{n-1}(x,y), Z^{n-1}(x-1,y), Z^{n-1}(x,y-1)) \\ &\quad + (Z(x,y) - Z^{n-1}(x,y)) \frac{\partial}{\partial Z(x,y)} f(E(x,y), Z^{n-1}(x,y), Z^{n-1}(x-1,y), Z^{n-1}(x,y-1)) \\ &\quad + (Z(x-1,y) - Z^{n-1}(x-1,y)) \frac{\partial}{\partial Z(x-1,y)} f(E(x,y), Z^{n-1}(x,y), Z^{n-1}(x-1,y), Z^{n-1}(x,y-1)) \\ &\quad + (Z(x,y-1) - Z^{n-1}(x,y-1)) \frac{\partial}{\partial Z(x,y-1)} f(E(x,y), Z^{n-1}(x,y), Z^{n-1}(x-1,y), Z^{n-1}(x,y-1)) \end{aligned} \tag{7}$$

Using Jacobi iterative scheme, we can finally obtain the simplified linear equation as (8).

$$\begin{aligned} Z^n(x,y) &= Z^{n-1}(x,y) - \frac{f(Z^{n-1}(x,y))}{\dfrac{df(Z^{n-1}(x,y))}{dZ(x,y)}} \\ \frac{df(Z^{n-1}(x,y))}{dZ(x,y)} &= \frac{(p+q)(p\cos\tau\tan\sigma + q\sin\tau\tan\sigma + 1)}{\sqrt{(1+p^2+q^2)^3}\sqrt{1+(\cos\tau\tan\sigma)^2+(\sin\tau\tan\sigma)^2}} - \cdots \\ &\qquad \frac{(\cos\tau\tan\sigma)+(\sin\tau\tan\sigma)}{\sqrt{(1+p^2+q^2)}\sqrt{1+(\cos\tau\tan\sigma)^2+(\sin\tau\tan\sigma)^2}} \end{aligned} \tag{8}$$

The Shah's Shape from Shading using linear approximation iteratively calculates the depth and surface normal information.

This Shape from Shading algorithm is applied to initial coarse DEM obtained from LOLA DEM. The pixel-wise intensity variation caused by small crater or boulders will be affected

to refine DEM since Shape from Shading utilized all the reflectance information for each pixel.

3. DATA DESCRIPTION

LRO Narrow Angle Camera Image

The LROC NACs are linear push broom scanner that consists 5064 elements CCD line array with size of 7 micron pixels. Two of LROC NAC are operated simultaneously. The NAC is designed to deliver 0.5m resolution panchromatic images covering a 2500m swath.

In the operation of LRO NAC, stereo images are collected by taking images on two different orbits. The total parallax angle of images from two trials is set to be greater than 12°. The average parallax angle is around 24°. The overlap of two images from Left NAC and right NAC is used to calculate the elevation data. Up to overlap layout, three or four stereo models are utilized. The amount of overlap and actual ground track are affected by local topography and orbit status [8].

LOLA Digital Elevation Model

LOLA is equipped on the LRO and is operated on the polar orbit with altitude 50km. The accuracy of LOLA is about 10cm. The data measurement is repeated in 28Hz. LOLA is a pulse detection time-of-flight altimeter. By measuring time-of-flight, it is able to estimate the depth information. The LOLA incorporates five-spot pattern to measure the precise distance to the lunar surface simultaneously. Each spots are of 57m distant away and 5m radius. LOLA also measures energy dissipativity, diffusivity to determine the reflectivity and roughness of lunar surface. The LOLA time-of-flight data is processed through the CODMAC (Committee on Data Management, Archiving, Computation) standard. The processed data is offered from NASA. The raw packet data from LRO is processed to the experiment data records (EDR) first. The EDR contains raw data from each instruments in LOLA and it should be converted to the reduced data records (RDR) to be properly analysed. The RDR contains physical quantity for the lunar data, yet not useful since only local data over the lunar surface exists. The gridded data records (GDR) is generated by fusing all RDR. The GDR is used for make a coarse DEM of region of interest. GDR subsists in several resolution models. The simplest LDEM-4 model has 7.58km resolution while the most precise model LDEM-1024 has 29.612m resolution. In this research, the LDEM over small area is necessary. The LDEM-1024 is used to create coarse DEM over small area on LRO NAC image.

Table 1 – LOLA GDR Classification [9]

Model	Pixel size	Number/size of tiles	bits/pixel
LDEM-4	7.5808 km	Global (1 tile)	16
LDEM-16	1.895 km	Global (1 tile)	16
LDEM-64	0.4738 km	Global (1 tile)	16
LDEM-128	0.2369 km	Global (1 tile)	16
LDEM-256	118.45 m	90° in latitude, 180° in longitude (4 tiles)	16
LDEM-512	59.225 m	45° in latitude, 90° in longitude (16 tiles)	16
LDEM-1024	29.612 m	22.5° in latitude, 45° in longitude (64 tiles)	16

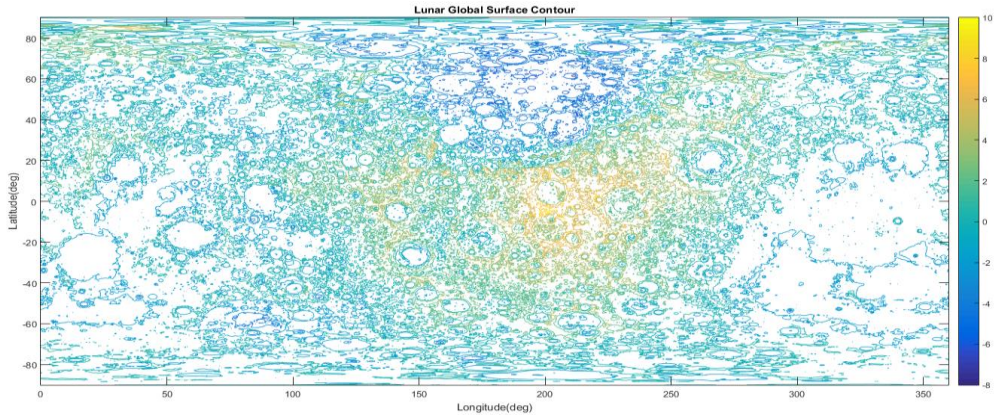

Fig. 2 – LOLA DEM created using GDR

4. SURFACE RECONSTRUCTION USING SFS

Results

To test the performance of Shape from Shading, the part of lunar surfaces are selected. Selection criteria is based on its topological complexity.

- An edge of crater Hyginus Caldera is selected because its slope makes altitude variation.
- A small crater is located near an edge of crater Hyginus Caldera.
- Small boulder exists over an edge of crater, which cannot be realized in LOLA data.
- Illumination direction is difficult to estimate solely based on image data.

Two LRO NAC image (0.5m/pixel) is used for Shape from Shading refinement (M111770178LR). The image is projected to a Mercator system and only part of two stereo images is used. The coarse DEM from LOLA data is utilized. LDEM-1024 model covering longitude 0°-30° and latitude 0°-15° is used. Coarse DEM is obtained by linear interpolation over the region of interest. The result of the high frequency DEM reconstruction for the NAC image M111770178LC is given like Fig. 3. The coarse DEM and refined DEM shows similar shape in large scale, however the high frequency altitude change caused by small crater and boulder are given as Fig. 3(d). The altitude variation caused by small crater is supplemented. Also, the effect of small boulder near the edge of crater causes very small, high frequency depth variation at the edge of crater. From the difference graph in Fig. 3(d) and Fig. 4(d), we can observe that the high frequency component of DEM is successfully reconstructed.

(a) Original NAC Image (M111770178LC)

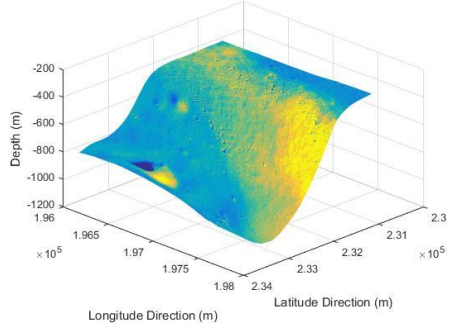

(b) Coarse DEM from LOLA data

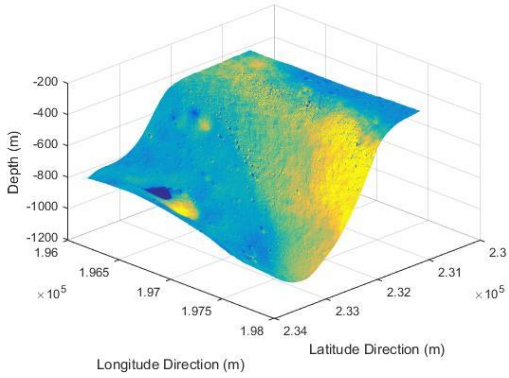

(c) Refined DEM using SfS

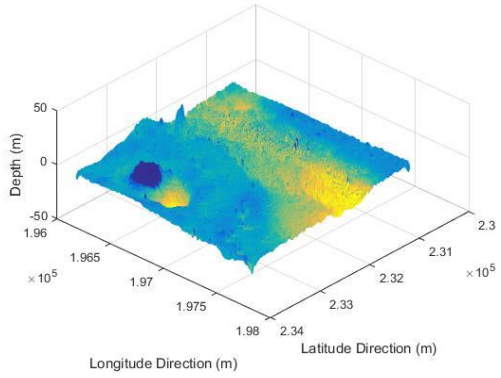

(d) Difference btw coarse and refined DEM

Fig. 3 – High Frequency Reconstruction of DEM of NAC Image M111770178L

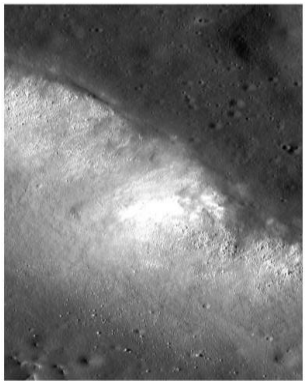

(a) Original NAC Image (M111770178RC)

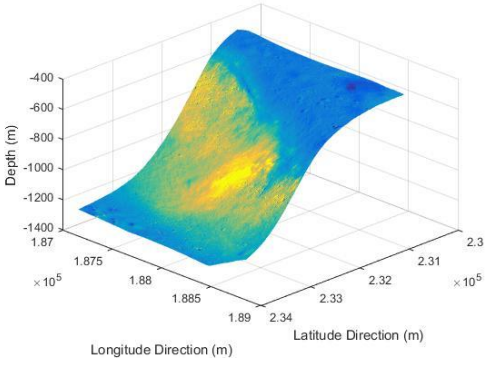

(b) Coarse DEM from LOLA data

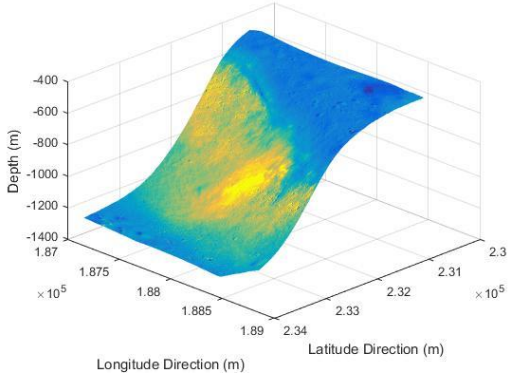

(c) Refined DEM using SfS

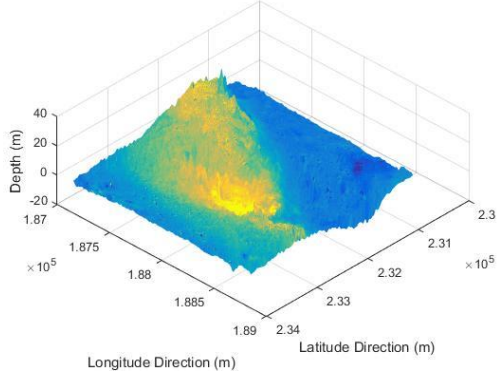

(d) Difference btw coarse and refined DEM

Fig. 4 – High Frequency Reconstruction of DEM over NAC Image M111770178R

5. CONCLUSIONS

In this paper, the Shape from Shading algorithm is applied to the high-resolution LRO monocular image and coarse DEM obtained from LOLA data. The Shape from Shading algorithm refines a DEM at a pixel level and successfully recovers the high frequency

information of terrain caused by small craters and boulders. Small crater that was not fully described in the LOLA DEM due to resolution limit of data is reflected into refined DEM. The depth difference between coarse DEM and refined DEM near this small crater is about 15m and it is reasonably explained. Also, small boulder at the edge of crater appears in refined DEM. Though information of small boulder appears, the depth variation due to these small boulder might be inaccurate because of small boulder size. The pixel intensity variation is large with only one or two pixels, which means depth change cannot be estimated accurately. The photoclinometric approach used in this paper basically assumes uniformity of albedo. However, the albedo over the lunar surface varies due to its component and roughness diverse point to point. Future work will be to include the albedo information for photoclinometry or to estimate the albedo and shape simultaneously.

ACKNOWLEDGEMENT

This work is supported by the National Research Foundation of Korea (NRF) grant funded by the Korean Government (MSIP). (No.2016M1A3A3A02017919).

REFERENCES

[1] M. J. Broxton, and L. J. Edwards, *The Ames Stereo Pipeline: Automated 3D surface reconstruction from orbital imagery*, Lunar and planetary science conference, League City, Texas, March 10-14, 2008.

[2] D. E. Smith, et al, The lunar orbiter laser altimeter investigation on the lunar reconnaissance orbiter mission, *Space science reviews* Vol. **150**, No.1-4, pp.209-241, 2010.

[3] F. Scholten, et al, GLD100: The near-global lunar 100 m raster DTM from LROC WAC stereo image data, *Journal of Geophysical Research: Planets*, Vol. **117**, No.E12, 2012.

[4] T. Tran, et al, *Generating Digital Terrain Models Using LROC NAC Images*, A special joint symposium of ISPRS Technical Commission IV & AutoCarto in conjunction with ASPRS/CaGIS, Orlando, Florida, Nov 15-19, 2010.

[5] A. Pentland, Shape information from shading: a theory about human perception, *Spatial vision*, Vol. **4**, No.2, pp.165-182, 1989.

[6] T. Ping-Sing, and M. Shah, Shape from shading using linear approximation, *Image and Vision computing*, Vol. **12**, No.8, pp.487-498, 1994.

[7] J. T. Barron, and M. Jitendra, *High-frequency shape and albedo from shading using natural image statistics*, 2011 IEEE Conference on Computer Vision and Pattern Recognition (CVPR), Colorado Springs, Colorado, Jun 20-25, pp.2521-2528, 2011.

[8] B. Wu, et al, *SHAPE AND ALBEDO FROM SHADING (SAfS) FOR PIXEL-LEVEL DEM GENERATION FROM MONOCULAR IMAGES CONSTRAINED BY LOWRESOLUTION DEM*, International Archives of the Photogrammetry Remote Sensing & Spatial Information Sciences, Prague, Czech Republic, Jul 12-19, pp.521-527, 2016.

[9] G. A. Neumann, et al, *Lunar Reconnaissance Orbiter Lunar Orbiter Laser Altimeter Archive Volume Software Interface Specification*, NASA, Ver 2.6, Dec 15, 2015.

[10] S. Herbort, A. Grumpe, and C. Wöhler, *Reconstruction of non-Lambertian surfaces by fusion of shape from shading and active range scanning*, 2*011 18th IEEE International Conference on Image Processing (ICIP)*, Brussels, Belgium Sep 11-14, 2011.